Analysis of the Comparative Responses of SMEI and LASCO

Andrew Buffington[*a], Jeff S. Morrill[b], P.Paul Hick[a], Russell A. Howard[b], Bernard V. Jackson[a] and David F. Webb[c]

[a]Center for Astrophysics and Space Sciences, Univ. of Calif., San Diego, CA, USA 92093-0424;
[b]Space Science Division, Naval Research Lab., Code 7660, Washington DC, USA 20375-5352;
[c]Institute for Space Research, Boston College; Also at: Air Force Research Lab., Space Vehicles Directorate; AFRL/VSBXS, Hanscom AFB, MA, USA 01731-3010

ABSTRACT

Surface-brightness responses of the SOHO-LASCO C3 coronagraph and of the Solar Mass Ejection Imager (SMEI) are compared, using measurements of a selection of bright stars that have been observed in both instruments. Seventeen stars are selected that are brighter than 4.5 magnitudes, are not known variables, and do not have a neighboring bright star. Comparing observations of these determines a scaling relationship between surface-brightness measurements from one instrument to those from the other. We discuss units of surface brightness for the two instruments, and estimate a residual uncertainty for the present scaling relationship.

Keywords: SMEI, LASCO, Photometry, Coronagraph, Calibration

1. INTRODUCTION

The LASCO coronagraphs[1] aboard the SOHO spacecraft have been delivering Solar coronal images since 1996; these have been used to study coronal mass ejections and other solar phenomena, and have measured the albedo of planets and comets. SOHO is located in orbit about the first Lagrange point L_1. The LASCO C3 coronagraph calibrations are described by Thernisien et al. (2006)[2] and reviewed in detail by Morrill et al. (2006).[3] Bright-star photometry was used in these previous articles to establish the C3 photometric calibration and measure its slight degradation with time (~0.4% per year).

The Solar Mass Ejection Imager (SMEI)[4,5] has been returning visible-light photometric data since launch and deployment to an 840 km circular polar orbit in January 2003. The SMEI data-analysis sequence converts these data into photometric individual-orbit sky maps covering nearly the entire sky. These maps have been used to track interplanetary disturbances,[6] observe high-altitude aurorae,[7] search for optical counterparts of gamma-ray bursts,[8] compile a catalog of coronal mass ejections (CMEs),[9] observe comet-tail disruptions,[10] and have also been employed for 3D density and velocity reconstruction of these CMEs.[11] This article presents results of a bright-star calibration of SMEI data, similar to that described for LASCO in references 2 and 3. Fifty-eight previously well-studied stars were used for the LASCO stellar calibration; these were brighter than 4.5th magnitude and passed through the C3 field of view each year.[3] To compare with SMEI photometric measurements, we further restricted stars from this list not to be variables and not to have a neighboring star brighter than 6th magnitude within 1° on the sky. Seventeen stars met this requirement, although one of these (ζ Tau) is somewhat variable but still useable for the present work. Photometric measurements of these seventeen stars by SMEI over the course of several years provides the present basis for relating LASCO C3 photometry to SMEI photometry.

2. LASCO C3 AND SMEI UNITS

Both the SMEI and the LASCO C3 coronagraph data originate as per-pixel electron counts gathered from the CCD detector within a given integration time. LASCO publications refer to these counts as data numbers (DN), whereas SMEI publications refer to these counts as analog-to-digital units (ADUs). In the present analysis, when photometrically

* abuffington@ucsd.edu; phone 858 534-6630; fax 858 534-0177

Solar Physics and Space Weather Instrumentation II, edited by Silvano Fineschi, Rodney A. Viereck
Proc. of SPIE Vol. 6689, 66890B, (2007) · 0277-786X/07/$18 · doi: 10.1117/12.734658

measuring a star whose point-spread function extends over several pixels or more on the CCD, the DNs or ADUs for LASCO or SMEI respectively are summed together, as though all the light had fallen on just one pixel.

To convert DN to a surface brightness, the LASCO data analysis chooses one C3 pixel as the angular subtense (see § 4.3.2 in reference 3): each pixel subtends ~2.4×10^{-4} square degrees. A pixel's observed sky brightness is expressed in terms of the ratio B/B_{sun}, where B_{sun} is the brightness that would be observed in that pixel were the LASCO C3 coronagraph to view the Sun's disk directly. This assumes that the absolute brightness of the Sun remains constant with time (see § 4.3.3 in reference 3). When analyzing coronal features near the Sun, this surface-brightness convention has the advantage that it automatically compensates for several percent variations in the distance of the SOHO spacecraft to the Sun. These distance variations result both from the spacecraft's location relative to the L_1 point, and from the Earth's orbital eccentricity. The angle subtended by the Sun's disk increases and diminishes with this changing SOHO-Sun distance, but the surface brightness at a given point within the Sun's disk does not change. Similarly, when LASCO observes a small patch of the corona at a given location near the Sun, its surface brightness does not change. Thus, as SOHO's position varies, the photometrically measured ratio B/B_{sun} requires no distance correction. Of course, the variable distance must still be taken into account when calculating "plane-of-the-sky" locations of observations relative to the Sun.

SMEI's optical design[4] causes the CCD-pixel subtense in the sky to vary somewhat over each camera's field of view. In a camera's narrow dimension of its field of view, a pixel subtends from 0.0547° to 0.0563°; in the long dimension the variation is from 0.0470° to 0.0493°. Slight differences exist from camera to camera. Also, as a star transits the field of view, the size of the point spread function (PSF) varies considerably. When an entire orbit's data are combined into a sky map, typically a dozen or more individual frames contribute to the average brightness seen at a given location. In composing the sky map, the data analysis preserves the average brightness seen by the camera. The resulting net PSF in a sky map is thus the combination of the individual-frame PSFs as the star transits the camera's field of view.[12] The average subtense for a SMEI pixel is 0.00269 square degrees, about ten times larger than that of the LASCO C3.

SMEI measures surface brightness over most of the sky. Here, with lines of sight at large angles to the Sun, the compensation described above becomes less useful, and a more common surface-brightness unit is an "S10", the equivalent number of 10th visual-magnitude solar-type stars per square degree (see § 13.3 in reference 13). Most of the 17 stars here are not solar-type G stars, but their spectral types are known and spectra are available.[14,15] Thus, each one's visual magnitude can be corrected by the ratio of the star's spectrum to that of the Sun, integrated over wavelength λ and multiplied by the appropriate CCD response and mirror reflectivity versus λ. The resulting "m_{smei}" serves then to connect SMEI's observed number of ADUs to the above S10 brightness scale.

3. DATA ANALYSIS & RESULTS

SMEI sky-map data currently span more than four years, and presently the mission continues. Response in all cameras, both for stars and diffuse background, is seen to diminish with time at about 1.6% per year. Radiation-damage buildup on the CCDs from exposure to the Earth's radiation bands (the South Atlantic Anomaly and auroral ovals) contributes, as may also loss of optical efficiency due to contamination buildup on the SMEI mirrors and CCD front surface.

Table 1 presents the seventeen selected stars described in the Introduction, including each star's numerical identifiers, name, spectral type, and visual magnitude m_v. Also included is the previously-mentioned scaled "SMEI magnitude", m_{smei} , and a similarly-calculated expected brightness B_{star}/B_{sun} , which is what LASCO would observe for this star if it were to have the SMEI bandpass in place of its own. For a SMEI sky map a brightness is determined for each of these stars by least-squares fitting the camera's PSF and a sloped background-light distribution to the surface-brightness observations near that star's location in the sky.[12] The ADUs above the background are summed to a total that is the response SMEI would have observed were all the star's light to fall upon a single pixel. Response from the cameras viewing nearest the Sun (camera 3) and antisolar (camera 1) are matched to the middle camera 2, which covers the most sky. Table 2 presents the summed-ADU results for the seventeen stars, together with the brightnesses expected from m_{smei}, in units of numbers of 10th magnitude stars, from

$$SMEI \quad brightness = (2.512)^{(10-m_{smei})}. \tag{1}$$

Figure 1 shows a scatter plot of table 2's expected SMEI brightness from equation (1) versus the observed ADUs for the seventeen stars; figure 2 shows table 1's B_{star}/B_{sun} versus the observed ADUs. The slope of figure 1 shows that a single

10^{th} magnitude star has 170 ADUs in summed response, which corresponds (each ADU here is 4.7 detected electrons)[4] to 800 electrons in a 4-second exposure for camera 2. Camera 1's value is about 825 electrons. The original SMEI design predicted about 1000 electrons. To determine the number of ADUs in a single S10 unit, multiplying the 170 ADUs by the 0.00269 subtense above yields: one S10 = 0.46 ADUs when spread over one square degree.

SAO #	HD #	Name	Spectral Type	m_v	m_{smei}	SMEI B_{star}/B_{sun}
76721	29763	τ Tau	B3V	4.28	4.57	2.49×10^{-10}
77336	37202	ζ Tau	B4IIIp	2.90-3.03	3.20-3.33	8.34×10^{-10}
79533	60522	υ Gem	M0III	4.06	3.37	7.40×10^{-10}
92680	11502	γ1,2 Ari	B9V+A	3.88	4.08	3.69×10^{-10}
93469	21754	5 Tau	K0II-III	4.11	3.97	4.56×10^{-10}
93954	28305	ε Tau	K0III	3.54	3.45	7.62×10^{-10}
98087	74442	δ Cnc	K0III	3.94	3.84	5.39×10^{-10}
98709	83808	ο Leo	A5V	3.52	3.81	6.08×10^{-10}
98964	87837	31 Leo	K4III	4.37	3.91	4.84×10^{-10}
99587	99028	ι Leo	F2IV	3.94	4.08	4.15×10^{-10}
110065	10380	ν Psc	K3III	4.44	4.05	4.21×10^{-10}
110543	15318	ξ2 Cet	B9III	4.28	4.58	2.53×10^{-10}
118804	98664	σ Leo	B9.5Vs	4.05	4.35	3.08×10^{-10}
128513	224617	ω Psc	F4IV	4.01	4.09	3.92×10^{-10}
138298	100920	υ Leo	G9III	4.30	4.21	3.73×10^{-10}
139189	114330	θ Virgo	A1V	4.38	4.67	2.36×10^{-10}
146585	219215	φ Aqr	M2III	4.22	3.37	7.37×10^{-10}

Table 1. The seventeen bright stars chosen to compare LASCO C3 and SMEI surface-brightness measurements. Spectral type and m_v are from reference 16. A corrected value for m_{smei} is derived from m_v and the spectral type, as described in the text. B_{star}/B_{sun} is calculated from the LASCO C3 values for these stars, but corrected for the differing SMEI and LASCO response curves.

Name	τ Tau	ζ Tau	υ Gem	γ1,2 Ari	5 Tau	ε Tau	δ Cnc	ο Leo	31 Leo	ι Leo	ν Psc	ξ2 Cet	σ Leo	ω Psc	υ Leo	θ Virgo	φ Aqr
ADUs ÷ 100	240	830	750	370	450	720	535	580	480	378	430	240	280	360	400	220	720
# 10^{th} mag stars	174	495	449	233	258	417	291	299	273	233	240	147	182	231	207	136	449

Table 2. Number of ADUs divided by 100 observed by SMEI for each of the seventeen stars, and the associated expected brightness for each. Values are calculated in units of number of 10^{th} magnitude solar-type stars (S10's), using m_{smei} and equation (1).

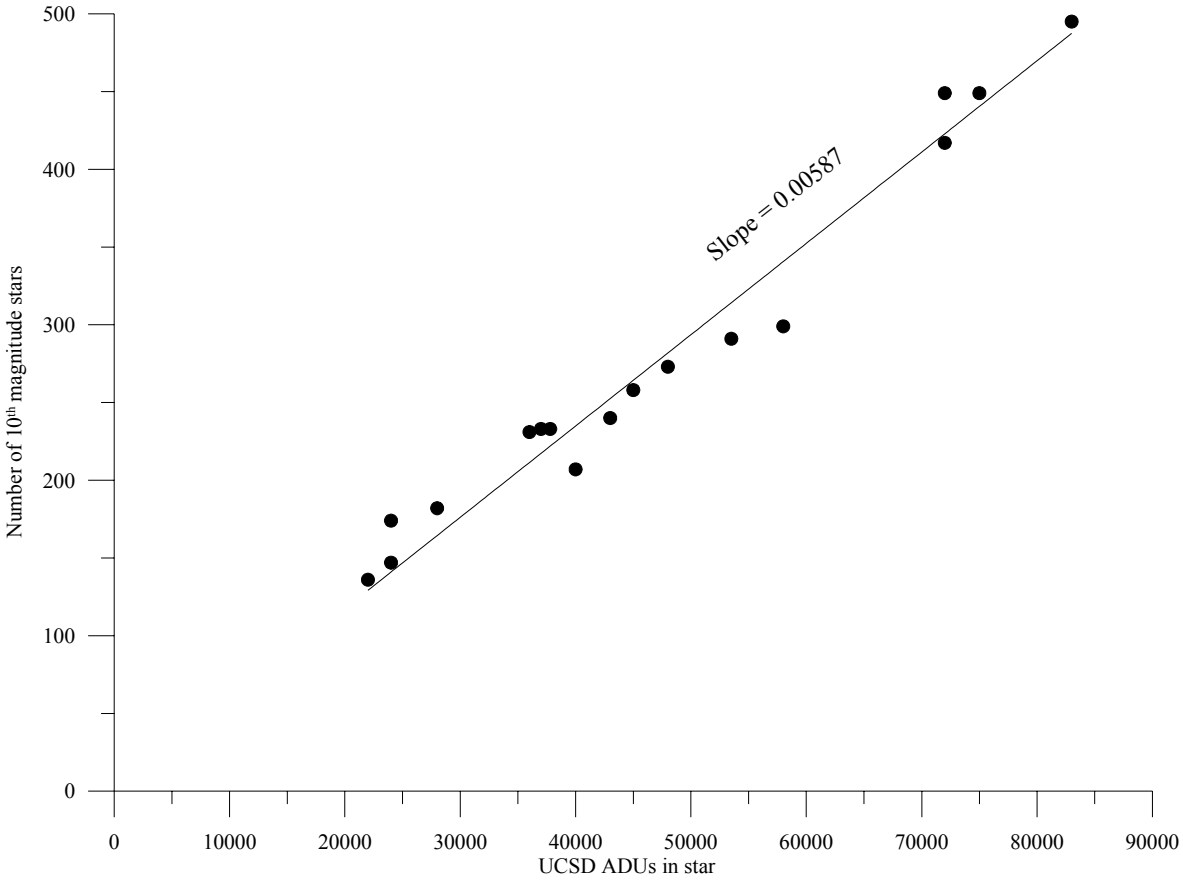

Fig. 1. Calculated expected equivalent number of 10^{th} magnitude stars versus total observed ADUs for SMEI. The SMEI data are averaged over four years for each of the seventeen stars.

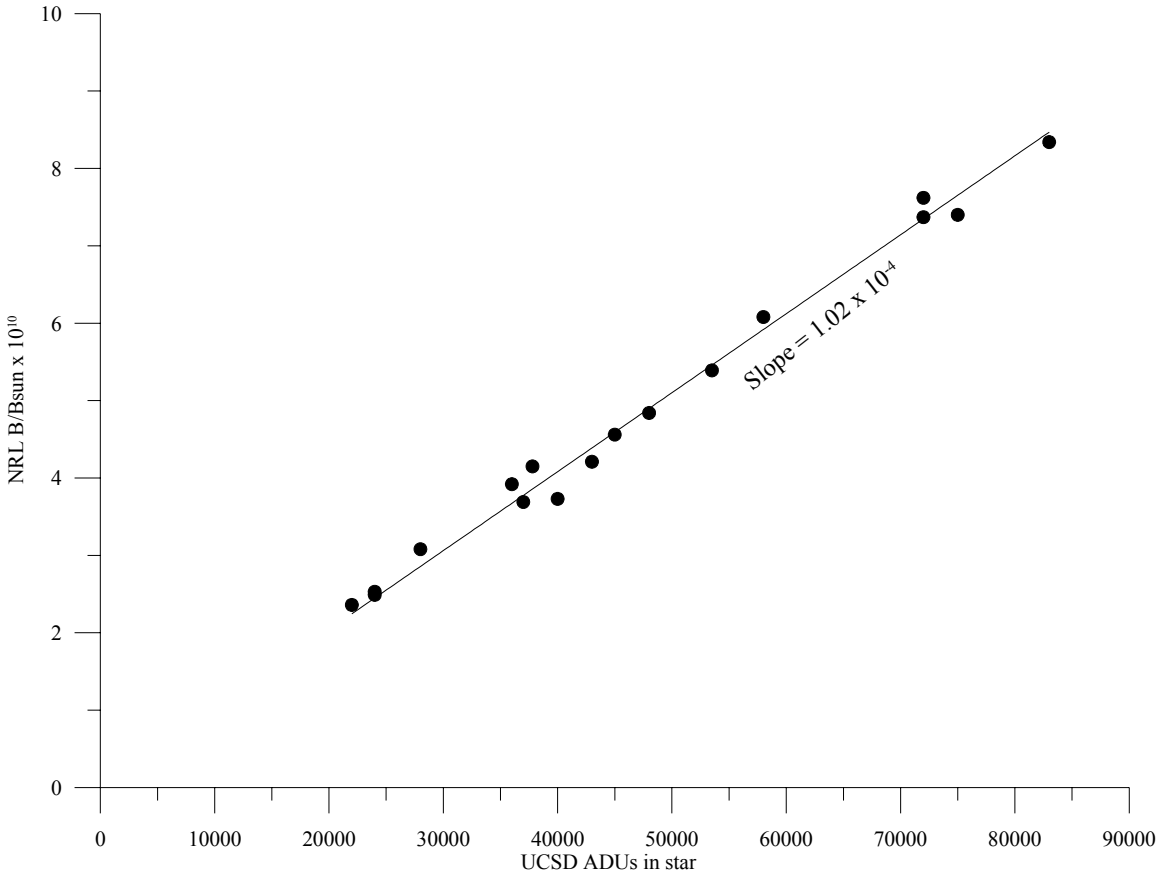

Fig. 2. Calculated expected B_{star}/B_{sun} versus total observed ADUs from SMEI.

The slope in figure 2 provides a means of converting SMEI stellar brightnesses to those of LASCO C3. The same number (times 10^{-10}), 1.02×10^{-14}, multiplies SMEI surface brightnesses to convert these to the LASCO brightness units. A further correction factor, usually only a few percent less than unity, is required when the star or other object being observed has a spectrum differing significantly from the solar spectrum. This factor is mostly caused by SMEI's added sensitivity to infrared wavelengths compared with LASCO. The change due to this correction is largest for red K- and especially M-type stars.

The rms residual scatter of the points in figure 1 is about 7%, which yields a formal error for the above conversion from ADUs to S10s, of about 2%. The rms scatter of the points in figure 2 is smaller than that of figure 1, about 4%, thus yielding a 1% formal error for the conversion between SMEI ADUs and LASCO B_{star}/B_{sun}. These formal-error values are probably low, since they do not include residual systematic-error contributions for either or both instruments' star fitting procedures,[3,12] and uncertainty in the spectral response of SMEI.

4. CONCLUSIONS

Conversion factors for LASCO C3 relative to SMEI photometric measurements have been determined. In particular, SMEI sky-map surface brightnesses in ADUs can be converted to LASCO C3 surface brightnesses by multiplying by 1.02×10^{-14}. The formal error in this determination based on the 17 stars used here is about 1%, but the actual uncertainty due to systematic-error contributions is probably 3 to 5%. The LASCO C3 calibration is based on 58 stars, somewhat more than the subset of 17 used here. A similar determination for SMEI is in progress, using about 5500 stars brighter than 6th magnitude, although the spectral types may be uncertain for some of the faintest of these. In any case, this more complete study may narrow the error from its value presented here. Finally, based on the photometry for these 17 stars, a surface brightness of one S10 in a SMEI sky map corresponds to 0.46 ± 0.02 ADUs.

ACKNOWLEDGEMENTS

We thank John M. Clover for much assistance in processing the SMEI data used for this study, and Mario M. Bisi for useful discussions and a careful reading of this manuscript. SMEI is a collaborative project of the U.S. Air Force Research Laboratory, NASA, the University of California at San Diego, the University of Birmingham, U.K., Boston College, and Boston University. The work at UCSD is partially supported by grants NSF ATM-0331513, NASA NNG05GM58G, and NASA NAG5-13453. This study was supported by the NASA Sun-Earth Connections GI program under grant NNGO5GF98G.

REFERENCES

1. Brueckner, G.E., R.A. Howard, M.J. Koomen, C.J. Korendyke, D.J. Michels, J.D. Moses, D.G. Socker, K.P. Dere, P.L. Lamy, A. Llebaria, M.V. Bout, R. Schwenn, G.M. Simnett, D.K. Bedford and C.J. Eyles, "The Large Angle Spectroscopic Coronagraph (LASCO)", *Solar Physics* **162**, 357-402, (1995).
2. Thernisien, A.F.R., J.S. Morrill, R.A. Howard and D. Wang, "Photometric Calibration of the LASCO-C3 Coronagraph Using Stars", *Solar Physics* **233**, 155-169, (2006).
3. Morrill, J.S., C.M. Korendyke, M. Andrews, D. Biesecker, G.E. Bruckner, E. Esfandiari, F. Giovane, R.A. Howard, M. Koomen, P. Lamy, A. Llebaria, D. Michels, D. Moses, S.P. Plunkett, N. Rich, A.F. Thernisien, A. Vourlidas and D. Wang, "Calibration of the SOHO/LASCO C3 White Light Coronagraph", *Solar Physics* **233**, 331-372, (2006) .
4. Eyles, C.J., G.M. Simnett, M.P. Cooke, B.V. Jackson, A. Buffington, P.P. Hick, N.R. Waltham, J.M. King, P.A. Anderson and P.E. Holladay, "The solar mass ejection imager (SMEI)", *Solar Physics* **217,** 319-347, (2003).
5. Jackson, B.V., A. Buffington, P.P. Hick, S.W. Kahler, E. Cliver, S. Price, J. Johnston, P. Anderson, P.E. Holladay, D. Sinclair, T. Kuchar, D. Mizuno, S.L. Keil, R. Radick, J. Mozer, R.C. Altrock, R. Gold, G.M. Simnett, C.J. Eyles, M.P. Cooke, N.R. Waltham and D.F. Webb, "The solar mass ejection imager (SMEI): the mission", *Solar Physics* **225,** 177-207, (2004).
6. Tappin, S.J., A. Buffington, M.P. Cooke, C.J. Eyles, P.P. Hick, P.E. Holladay, B.V. Jackson, J.C. Johnston, T. Kuchar, D. Mizuno, J.B. Mozer, S. Price, R.R. Radick, G.M. Simnett, D. Sinclair, N.R. Waltham, and D.F. Webb, "Tracking a Major Interplanetary Disturbance with SMEI", *Geophys. Res. Lett.*, **31**, L2802-2805, doi:10.1029/2003GL018766, (2004).
7. Mizuno, D., A. Buffington, M.P. Cooke, C.J. Eyles, P.P. Hick, P.E. Holladay, B.V. Jackson, J.C. Johnston, T. Kuchar, J.B. Mozer, S. Price, R.R. Radick, G.M. Simnett, D. Sinclair, J. Tappin, and D.F. Webb, "Very High-Altitude Aurora Observations With the Solar Mass Ejection Imager", *J. Geophys. Res.*, **110**, A07230, doi:10.1029/2004JA010689, (2005).
8. Buffington, A., D.L. Band, B.V. Jackson, P.P. Hick, and A.C. Smith, "A Search for Early Optical Emission at Gamma-Ray Burst Locations by the Solar Mass Ejection Imager (SMEI)", *Astrophys. J.,* **637**, 880, (2006).
9. Webb, D.F., D. R. Mizuno, A. Buffington, M.P. Cooke, C.J. Eyles, C.D. Fry, L.C. Gentile, P.P. Hick, P.E. Holladay, T.A. Howard, J.G. Hewitt, B.V. Jackson, J. C. Johnston, T. A. Kuchar, J. B. Mozer, S. Price, R. R. Radick, G. M. Simnett, and S. J. Tappin, "Solar Mass Ejection Imager (SMEI) Observations of CMEs in the Heliosphere", *J. Geophys. Res.*, **111**, A12101, doi:10.1029/2006JA011655, (2006).
10. Kuchar, T.A., A. Buffington, C.N. Arge, P.P. Hick, T.A. Howard, B.V. Jackson, J.C. Johnston, D.R. Mizuno , S.J. Tappin , D.F. Webb, "Observations of a Comet Tail Disconnection Induced by CME Passage", *J. Geophys. Res.*, *submitted,* (2007).
11. Jackson, B.V., Buffington, A., Hick, P.P. and Wang, X., "Preliminary 3D Analysis of the Heliospheric Response to the 28 October 2003 CME using SMEI White-Light Observations" *J. Geophys. Res.*, **111**, A04S91, doi:10.1029/2004JA010942, (2006).
12. Hick, P.P., Buffington, A., and Jackson, B.V., "A Procedure for Fitting Point Sources in SMEI White-Light Full-Sky Maps", *Proc. SPIE* **6689**, this meeting, immediately following this paper, (2007).
13. "Allen's Astrophysical Quantities, fourth edition", edited by A.N. Cox, AIP Press, Springer Verlag, New York (2000).
14. Pickles, A.J., "A Stellar Spectral Flux Library: 1150 - 25000 Å", *Publ. Astron. Soc. Pacific*, **110**, 863, (1998).
15. Neckel, H., and Labs, D., "The Solar Radiation between 330 and 12500 Å", *Solar Physics*, **90**, 205-258, (1984).
16. Hirshfeld, A. and Sinnott, R.W., "Sky Catalogue 2000.0", Cambridge Press, New York, (1982).